ISSN: 2230-9926

*Available online at http://www.journalijdr.com*

IJDR

*International Journal of Development Research*
*Vol. 10, Issue, 09, pp. 40427-40432, September, 2020*
https://doi.org/10.37118/ijdr.19878.09.2020

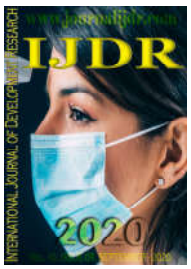


RESEARCH ARTICLE OPEN ACCESS

# SATELLITE-DERIVED BATHYMETRY IN THE TURBID AND SHALLOW WATERS OF THE BANDAMA ESTUARY (COTE D'IVOIRE) USING A LANDSAT 7 ETM+ MULTISPECTRAL IMAGE

***[1]Jeanne Maffoué Kouadio, [2]Patrick Boua Yahiri, [3]Abaka Brice Mobio and [4]KouadioAffian**

Centre Universitaire de Recherche et d'application en Télédétection (CURAT), Université Félix Houphouet Boigny, 22 BP 801 Abidjan 22, Côte d'Ivoire

**ARTICLE INFO**

***Article History:***
Received 17th June 2020
Received in revised form
14th July 2020
Accepted 21st August 2020
Published online 30th September 2020

***Key Words:***
Satellite-derived bathymetry,
Landsat-7 ETM+,
Bandama's estuary,
Côte d'Ivoire.

****Corresponding author:***
***Jeanne Maffoué Kouadio***

**ABSTRACT**

In shallow waters, traditional bathymetric methods such as acoustic and LIDAR (Light Detection And Ranging) systems are accurate; however they are constrained by high operational costs, logistic difficulties and limited spatial coverage. Shallow water depth estimation using passive remote-sensing method is an attractive alternative as it provides a time- and cost-effective solution to water depths estimation. The paper highlights the application of incorporating satellite remote sensing techniques to extract bathymetry information from the freely downloadable Landsat-7 ETM+ satellite images. This paper compares the two of the most commonly used methods, Stumpf and Lyzenga to estimate water column depth in Bandama estuary.The Lyzenga's model achieved root mean square error (RMSE) of 1.91 m, while Stumpf's model delivered RMSE of 3.09 m. The absolute differences between known depths and estimated depths (MAE)was 1.44 m concerning Lyzenga's model, whilst Stumpf's model obtained MAE of 2.59 m.In general, the Lyzenga's model is more robust than the Stumpf's model in the study area. The geographical distributions of model residuals are mapped as a basis for comparing the performance of the bathymetric models. The map of model residuals revealed a tendency for negative residuals in shallower areas and positive residuals in deeper areas.

***Copyright © 2020, Jeanne Maffoué Kouadio et al.*** *This is an open access article distributed under the Creative Commons Attribution License, which permits unrestricted use, distribution, and reproduction in any medium, provided the original work is properly cited.*

**Citation:** ***Jeanne Maffoué Kouadio, Patrick Boua Yahiri, Abaka Brice Mobio and KouadioAffian. 2020.*** "Satellite-derived bathymetry in the turbid and shallow waters of the bandama estuary (cote d'ivoire) using a landsat 7 etm+ multispectral image*", International Journal of Development Research*, 10, (09), 40427-40432.

## INTRODUCTION

Accurate and updated bathymetries are crucial for planning near-shore structure activities such as engineering work, port management, pipeline laying, fishing, dredging operation, oil drilling, aquaculture, maritime defence, and it is also significantly important to determine the underwater topography and movement of sediments and to generate hydrographic charts for safe transportation. Furthermore, bathymetric information is important for driving predictive modelling which makes it possible for the proactive management of impacts on near-shore marine habitats (Bramante *et al*., 2013).The traditional bathymetric surveying of shallow sea water is frequently based on ship-borne echo sounding and airborne LIDAR which provide high accuracy bathymetry. However, the cost and logistical difficulties of obtaining nearshore bathymetry using these methods makes survey updates rare. In shallow water areas, ship borne sounding is performed by using a single or multi-beam echo sounder system which is only capable of determining the depth accurately but encountered high operational risk due to limited navigation space, the shallowness of the water, etc. Moreover shipborne sounding is time consuming operation. Regarding LIDAR, this technique is expensive operational cost for many applications, especially when updates of a bathymetric data set are required with any frequency (Minghelli-Roman *et al*., 2009). Furthermore, some limitations associated with LIDAR are the time consuming, complex procedures, and limitation to relatively small areas due to the airborne nature (Figueiredo *et al*., 2015). The highly dynamic nature of near-shore regions leads to frequent changes in bathymetry that are required to be monitored at periodic intervals, hence, the survey should be carried out frequently. Ever since the 1970s, satellite remote sensing technology has been gradually adopted as an alternative tool to map the bathymetry of the ocean, because of its synoptic view, cost- and time-effectiveness and repeatability. The dynamic nature of the remote sensing makes it suitable to map bathymetry for studies of the fast-changing coastal environment (Zhang *et al*., 2008).Bathymetry retrieval using remote sensing technology is new topic and still less

explored in Cote d'Ivoire, particularly in the estuary of the River Bandama. This neashore coastal area presents seasonal shallows disrupting navigation of fishing boats. SDB can be used as an alternative to update the bathymetry data in order to regularly locate these shallows. This could be very helpful for fishing and nautical activities. Therefore, this present study is the first one which examines SDB approach to estimate the depth of turbid and shallow waters of the Bandama estuary.The objective of this paper is to evaluate the contribution of the visible and NIR (Near Infra-Red) bands of Landsat 7 ETM+ in the estimation of sea depths. Multi spectral and spatial image resolution was tested in estuary of River Bandama's shallow and turbid waters by using the well-known and time-tested Lyzenga and Stumpf methods (Jawak *et al*, 2015). To achieve this main objective, two specific goals have been considered, particularly : i) the assessment of the accuracy of each method using statistical indices (coefficient of determination ($R^2$), Root Mean Square Error (RMSE), Mean Absolute Error (MAE)) ; ii) Mapping model residuals, in order to locate the under- or over-prediction areas of the models.

## STUDY AREA AND METHODOLOGY

**Study area:** The bathymetric models were applied to Bandama estuary in Grand-Lahou (Côte d'Ivoire). It is located in the eastern side of Grand-Lahou lagoon, between 4°26 N and 5°20 N latitudes and 4° 20 W and 5°20 W longitudes. The Bandama estuary presents three channels separated by shoals emerging in period of low water level or by small islands (Figure 1). These channels and shallows are covered by fine and medium sands (Abé *et al*., 1993). Topographic surveys (Wognin *et al*. (2008), Abé *et al*. (1993), Hauhouot and N'douffou, 2009) etc.) show significant migration of the river mouth from East to West accompanied by severe near-shore coastal erosion. Tides in the area are semi-diurnal, with average ranges of 0.6 m and 1.4 m for neap and spring tides, respectively. The mean sea level is 0.78 m. Wave energy is moderate with an annual offshore significant wave height (Hs) which fluctuates between 1.28 and 1.65 m and a range of 9.4 à 10.6 s for peak period (Tp).

**The multispectral imagery and bathymetric data:** The bathymetric models were calibrated using echo sounding data. The survey of the bottom was accomplished through 59807 measurements of depths (from 0 m to 19 m). The depth soundings are in meters and are referenced to UTM (zone 30) system and WGS84. The bathymetric data were subset into two separate calibration and validation datasets, eachcomprising half of the survey points, using thesubset features tool in ArcGIS 10.5 (Geostatistical Analyst Tools), which randomly assigns points to either of the data subsets. For this study blue (B1), green (B2), red (B3) and NIR (B4) bands of Landsat 7 satellite imagery are used. The image was acquired on 6th January, 2011 at 10:27:27.76 (UTC Time) with spatial resolution of 30m. The reason for applying blue, green and red band in the coastal environment is that radiance in the blue band (450 – 515 nm) decreases more rapidly with depth than radiance in the green band (525 – 605 nm) and red band (630 – 690 nm). Generally, light at wavelengths above 700 nm has a very low transmittance in sea water. Therefore water appears dark and the land appears bright. For this reason, the NIR band (750 – 900 nm) is used for distinguishing water from land. Landsat imagery was selected because it is freely available and all imageries are referenced to WGS84.

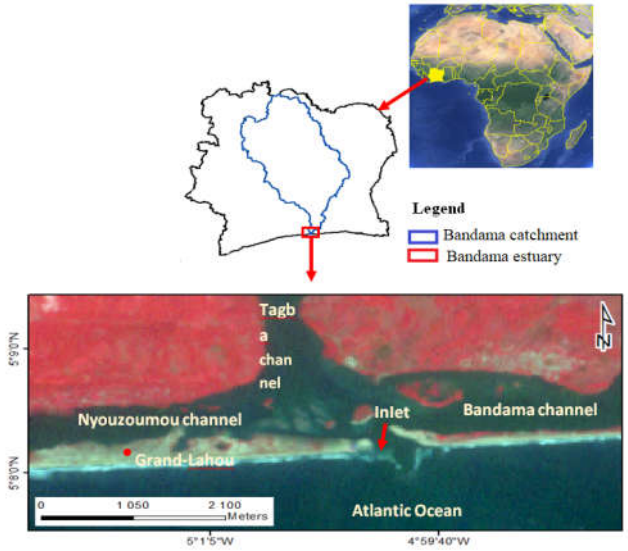


**Figure 1. False color composite (R: 4, G: 3, B: 2) of location of Bandama river estuary. R: 4, G: 3, B: 2 shows a color composite image from three bands (blue, green and infra-red bands)**

**Processing software:** ENVI version 5.1 image processing software from ITT Solutions was used for the pre-processing (radiance conversion, atmospheric correction, tidal correction, water separation) of the ETM+ imagery. ArcMap software version 10.5 with the support of 3D Analyst Tool was the main software used for the processing stage. R version 3.4.3 (R Core Team, 2017) was the supporting software utilised for accuracy analysis and statistical exploration.

## METHODOLOGY

This section outlines the processes being adopted in this study to derive nearshore bathymetry from the remotely sensed satellite imagery. They included radiance conversion, atmospheric correction, tidal correction, water separation and the implementation of bathymetry inversion models. In this paper we ignore the possible effects of sunlight, ETM+ image of the study area is clear of sunlight.

**Atmospheric Correction:** For the present paper, atmospheric corrections were performed using the Dark Object Subtraction (DOS) method. DOS assumes that dark objects or pixel (e.g., deep water and shadows) have near-zero-percent reflectance. Thus, the signal recorded by the sensor from these features includes a substantial component of atmospheric scattering, which must be removed (Chavez, 1988). The atmospherically corrected pixel value *Rac* is then:

$$R_{ac} = R_i - R_{dp}$$

Where $R_i$ is the initial pixel value and $R_{dp}$ the dark pixel value.

**Water Separatio**

Before estimating nearshore bathymetry it is important to separate land from water. For this purpose, NIR band is used due to the appearance of water in dark and land in bright (Figure 2a). The land/water threshold value is obtained by drawing a linethat crosses from land (bright areas) into the water (dark areas). The values above 0.10 represent land whereas low values below 0.10 represent water (Figure 2b).

The obtained threshold value of 0.10 is used to separate land from water.

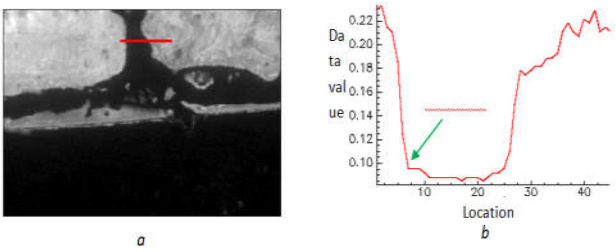


**Figure 2. Transect (a) and Threshold value (b) to separate the land from water**

**Bathymetry Inversion Models:** Several methods have been developed to derive bathymetry data from satellite images. This study adopted the two (2) of the most commonly used methods, Stumpf and Lyzenga to estimate water column depth in Bandama estuary. Both models apply the fundamental principle of Beer-Lambert Law. According to this principle, light is attenuated exponentially with depth in the water column. This principle is explained mathematically as follows:

$$L(z) = L(0)exp(-2Kz)$$

K is the attenuation coefficient and z is the depth, L(z) is downward irradiance at z m depth and L(0): downward irradiance at just below the water surface. Lyzenga (1978) showed that the relationship of observed reflectance (or radiance) to depth and bottom albedo could be described as:

$$R_w = (A_b - R_\infty)exp(-gz) + R_\infty$$

Where $R\infty$ is the water column reflectance, if the water is optically deep, $Ab$ is the bottom albedo, $z$ is the depth, and $g$ is a function of the diffuse attenuation coefficients for both downwelling and upwelling light.

**Lyzenga Model:** This model was introduced by Lyzenga (1978) and developed through a series of Lyzenga's findings (Doxani *et al*., 2012). Lyzenga described the relationship between an observed reflectance Rw and the corresponding water depth z and bottom reflectance $A_b$ as it is expressed in equation 3. Equation 3 can be rearranged to describe the depth in terms of the reflectance's and the albedo as

$$z = g^{-1}[ln(A_b - R_\infty) - ln(R_w - R_\infty)]$$

$$Z = a_0 + a_iX_i + a_jX_j$$

Where $X_i = ln[R_w(\lambda_i) - R_\infty(\lambda_i)]$

$$X_j = ln[R_w(\lambda_j) - R_\infty(\lambda_j)]$$

$R_w(\lambda_i)$ : observed reflectance for band $\lambda_i$ after atmospheric correction.

$R_\infty(\lambda_i)$ : column reflectance of optically deep water for band $\lambda i$.

$a_0$, $a_i$... $a_j$ = coefficients determined through multiple regression using known depths and the corresponding reflectances, they are considered to be constant coefficients over the entire scene. The algorithm can be expressed for n bands as:

$$Z = a_0 + \sum_{i=1}^{n} a_i ln[R_w(\lambda_i) - R_\infty(\lambda_i)]$$

$n$ is the number of bands, in this study, the blue band (B1), green band (B2), red (B3) and NIR band (B4) of Landsat 7 ETM+ have been used to apply linear band models.

**Stumpf Model:** Stumpf *et al*. (2003) proposed an alternativemodel to overcome the drawbacks of changing substrate albedo in deriving bathymetry information (Jawak *et al*., 2015). The algorithm assumes that the effects of substrate albedo are minimized using two bands to derive the depth. Low-absorption bands will have reflectance values that decrease with depth more slowly than high-absorption bands. Thus, the ratio of a low absorption band to a high absorption band should display a linear increase with depth when both are log-transformed. Equation 7 below demonstrates the Stumpf's algorithm:

$$Z = m_1 \frac{ln(n(L_{LO}))}{ln(n(L_{HI}))} - m_0$$

Where $m_1$ is a tunable constant defining the slope of the relationship between the ratio and depth, $m0$is an offset for zero depth (Z = 0). $L_{LO}$ and $L_{HI}$ are observed radiance of low-absorption and high-absorption bands respectively, $n$ is a large constant used to ensure positive logarithm values under any condition and that the ratio will produce a linear response with depth (Stumpf *et al*., 2003). In this present work, thevalue of $n$ was set to 1000. Stumpf *et al*. (2003) showed that the model is insensitive to threefold changes in the value of $n$ ($n$ varying from 500 to 1,500).

**Mapping Model Residuals:** Model residuals were mapped as a simple way to visually examine the spatial distribution of the performance of bathymetric estimations. A point shapefile was produced to depict the model residuals in their geographical location at each site. This shapefile was then interpolated to a continuous raster surface using a kigring algorithm. Kriging was selected because it has emerged as an optimal spatial interpolation method for mapping point values of residuals in model predictions (Kyriakidis *et al*., 2001). The resultant layer was then used as a visualization tool for examining the spatial distribution of error associated with the bathymetric estimations.

## RESULTS AND DISCUSSION

## RESULTS

### Model training

The visible and NIR bands of ETM+ image and 29904 bottom depth points of the training data set were used to calibrate the bathymetric inversion models. A preliminary test was performed in order to evaluate the significance of visible and NIR bands of ETM+ in Stumpf *et al*. and Lyzenga models. Different band ratios were tested to select low-absorption and high-absorption bands, agreement with ratio of blue band (B1, low-absorption band) to NIR band (B4, high-absorption band) of ETM+ having greater correlation with depth than the more conventional blue–green ratio (B1/B2) (Table 1).

**Table 1. Coefficient of determination ($R^2$) to select low-absorption and high-absorption bands**

| Band Ratio | B1/B2 | B1/B3 | B1/B4 |
|---|---|---|---|
| $R^2$ | 0.06 | 0.15 | 0.56 |

The three visible wavelength bands (blue, green and red) and the NIR band of ETM+ were used to train Lyzenga's algorithm. Thereafter, the four bands were removed successively in order to determine the significance of each band in Lyzenga's model. Successive removal of blue, green and red band resulted in slight decrease in accuracy ($R^2$ = 0.9091, $R^2$ = 0.9045 and $R^2$ = 0.9003 for the removal of blue band, green band and red band respectively, where $R^2$ is the coefficient of determination between the true measured water depth value and the corresponding pixel of log-transformed radiance values). The removal of the NIR band resulted in significant decrease in accuracy of the model ($R^2$ value decreased from 0.91 to $R^2$ = 0.6989). The parameters of Stumpf and Lyzenga algorithms are displayed in Table 2.

**Table 2. Parameters used with the two physically based models, as defined in Equations (6), (7)**

| Parameters | | | | | | | |
|---|---|---|---|---|---|---|---|
| | $a_0$ | $a_1$ | $a_2$ | $a_3$ | $a_4$ | $m_0$ | $m_1$ |
| Lyzenga | -29.29 | 0.52 | -1.41 | -1.73 | -5.06 | | |
| Stumpf | | | | | | -172.54 | 159.054 |

## Validation

The assessment of accuracy is made by comparing the SDB with 29903 bottom depth points of the validation dataset. The accuracy of each model is assessed using two simple statistical parameters along with the coefficient of determination $R^2$, root mean square error (RMSE) and mean absolute error (MAE). The coefficient determination between the model-predicted depths and the reference bottom depths is 0.77 and 0.90 for Stumpf's model and Lyzenga's model respectively. Regarding the statistical analysis, Lyzenga's model obtains RMSE of 1.91 metres while Stumpf *et al.*'s model delivers RMSE of 3.09 metres. The absolute difference between known depths and estimated depths (MAE) is equals to 1.44 meters for Lyzenga's model, whilst the MAE obtains by Stumpf's model is 2.59 meters.Analysis of the statistical parameters indicates that the Lyzenga model is more accurate than the Stumpf model. This results in a high value of the coefficient of determination and low values of RMSE and MAE obtained by the Lyzenga model compared to those obtained by the Stumpf model. This could be explained by the number of spectral bands (4 bands including blue, green, red and PIR) used in the Lyzenga model. Indeed, in theory the number of significantly different bottom types and water masses that this algorithm takes into account is directly proportional to the number of bands used in order to produce more accurate results over heterogeneous waters. The SDB maps (Figure 3a and Figure 3b) suggested that Stumpf's model underestimates depth in deeper areas whereas Lyzenga's model overestimates depth in deeper areas.

The Figure 3a and Figure 3b also show that Lyzenga's and Stumpf's models deliver negative values of depth in very shallow areas, with a large range of negative values (0 m to -7 m) obtained by Stumpf's model compared to those obtained by Lyzenga's model (0 m to -3 m). These very shallow areas are characterized by suspended sediments which can cause the discrepancies between *in-situ* and derived depth values. The negative values of depth show that both Lyzenga's and Stumpf's models fail to derive bathymetry in the very shallow and turbid waters of the estuary. Bathymetric maps produced by the models are displayed in Figure 3.

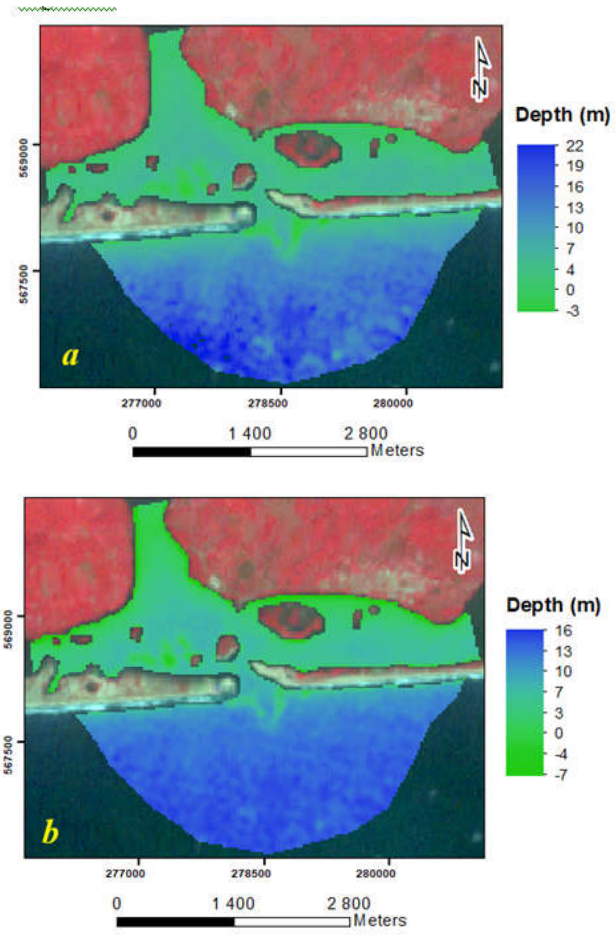


**Figure 3. Bathymetric maps derived from ETM+ image: (*a*) Lyzenga's model; (*b*) Stumpf's model.**

The spatial distribution of residuals also shows that Lyzenga's model appeared to perform better because its residuals were constrained around a narrower range of values (-5 to 7 m) (Figure 4a) compared to those of Stumpf's model (-7 to 10 m) (Figure 4b). A detailed investigation using theresidual depth map (Figure 4b) indicates that spatial heterogeneity was not effectively addressed by Stumpf's model. The residuals would be randomly distributed in space if both Lyzenga and Stumpf inversion models were robust to the bottom type variation. The residual map of Stumpf's model displays more distinctive geographical structure. In shallower regions, negative residuals tend to be located nearby each other and form several clusters in space. This involves that Stumpf's model overestimates the water depth in shallow areas. The positive residuals form clusters in deeper areas where the model underestimates the water depth. Concerning Lyzenga's model, the residuals are randomly distributed in space (Figure 4a).

Nonetheless, the Figure 4a displays a spatial distribution of residuals which is relatively unstructured with little discernible pattern of underestimate or overestimate of depth across shallower and deeper zones. The spatial clustering of positive and negative residuals suggests that the model is inclined to overestimate the water depth for some bottom types and to underestimate the water depth for other bottom types.

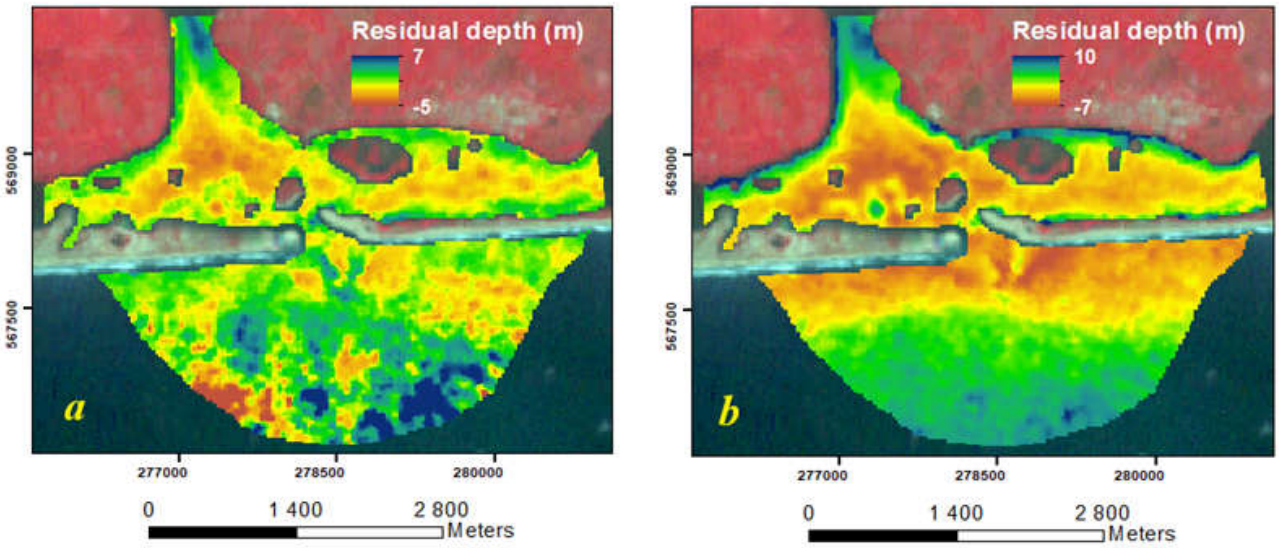


**Figure 4. Mapsofthespatial distribution of residuals: (*a*) Lyzenga's model; (*b*) Stumpf's model**

## DISCUSSION

Several studies (Jagalingam *et al*. 2015, Zhang *et al*. 2008,Stumpf *et al*. 2003, Evagorou *et al*. 2019, etc.) use band ratio of blue (low-absorption band) to green (high-absorption band) to implement Stumpf *et al* model in relatively clear water. However, in the turbid waters of Bandama estuary a band ratio of blue band (low-absorption band) to a band with a wavelength greater than those of the green band like red or NIR band(high-absorption band) have greater correlation with depth than the blue-green ratio. These results corroborate those obtained by Bramante *et al*. (2014) in Singapore's shallow turbid waters which found that ratios of the World view-2 satellitecoastal blue band (low-absorption band) to its yellow band (high-absorption band) having greater correlation with depth than the more conventional blue-green ratio.Therefore, the band ratio B1/B4 was selected to implement Stumpf *et al* model.Concerning Lyzenga's model, the adjunction of NIR band to the three visible bands of ETM+ resulted in significant increase in accuracy of the model ($R^2$ value increased from 0.69 to $R^2$ =0.91). According toHala *et al*. (2017) the NIR band affect Lyzenga's model for better estimation of depth values in coastal shallow waters. From all this, it follows that the NIR band of ETM+ is crucial for deriving bathymetry in shallow and turbid waters. In general, Lyzenga *et al* and Stumpf *et al* models, successfully produced decent results($R^2$ is 0.77 and 0.90 for Stumpf's model and Lyzenga's model respectively) in this turbid waters region. These two algorithms are found to be superior to accurately determine the shallow depth in highly turbid waters(Jawak *et al*, 2015). Stumpf model has less number of empirical coefficients which makes the method simple to use and more stable over broad geographic areas.However, Lyzenga linear band model employs two or more bands, which allows to take to account different bottom types and water masses in heterogeneous environment like in the estuary of Bandama. This particularity of Lyzenga model makes it provide better results than Stumpf model in the study area. The underestimation and overestimation problem could be tied to water quality across the study area. Indeed, the acquisition date of the images coincides with the great dry season in Bandama estuary. The phytoplankton tend to proliferate during this season (Komoé *et al*, 2009).

The vertical distribution of phytoplankton could cause variance in attenuation coefficients with depth (Bramante *et al*, 2013). This vertical stratification of phytoplankton could lead to some discrepancies in light attenuation with depth in the water column. Thus, the two physics-based models could deliver some biases when deriving depth. This could explain the bias towards overestimation that seems present in the Stumpf and Lyzenga models in shallower areas and the underestimation bias in deeper areas. Moreover, the Bandama River discharges cause high suspended sediment concentrations in the estuary. Water turbidity caused by suspended sediment limits the penetration of light. In these instances, the number of photons detected by the sensor that have interacted with the seafloor will become negligibly small. At this point, there will be no information for the estimation of bathymetry (Hamylton *et al*., 2015). The negative values of depth delivers by Stumpf's model in shallow areas could be due to the disadvantage of the atmospheric correction used in this study (dark pixel subtraction). A drawback appears in cases where the bottom reflectance is lower than the dark pixel value, for instance when the bottom is covered with sea grass, the difference in equation (1) becomes negative. Consequently equation (6) and equation (7) cannot be satisfied as the natural logarithm of a negative quantity is not defined. The resulting signal is negative, resulting in an imaginary value when log-transformed (Bramante *et al*., 2013). This explains negative values of depth encountered in shallow areas when applying Stumpf's algorithm. In the aforesaid circumstances, Lyzenga's algorithm fails to derive bottom depth in certains locations of the study area.

### Conclusion

This study examines usability of satellite derived bathymetry in estuary of Bandama's shallow and turbid waters. Throughout this experiment,a comparison ofLyzenga and Stumpf models reveals that Lyzenga *et al*. model provides the best performance of the two models. Although the Lyzenga's model appeared to perform better than the Stumpf's model, both were subject to the same depth limitations, which are likely governed by the water quality and bottom type. Globally, Lyzenga *et al* and Stumpf *et al* models produced reasonably good depth estimates in these shallow coastal

waters. The NIR band proved to be most effective for deriving bathymetry in shallow and turbid waters of Bandama estuary. Spatial error demonstrated that the mapping of model residuals is a useful tool for the exploration of error in bathymetry estimation models. This study considers as a part of a larger effort to evaluate various cost effective, relatively accurate and practical bathymetry survey methods. Also, by stacking Landsat 7 imagery time series with historical data, it is possible to distinguish the seabed topography.

## REFERENCES


Abe J, Bakayoko S, Bamba SB, Koffi, KP1993. Morphology and Hydrodynamic in the Bandama Inlet. Jour. Ivoir. Océanol. Limnol. Abidjan. Vol. 2 n°2, pp. 9-15.

BramanteJF, Raju DK, Sin TM 2014.Multispectral Derivation of Bathymetry in Singapore's Shallow, Turbid Waters. *International Journal of Remote Sensing*, 34:6, 2070-2088.

Chavez PS. Jr 1988. An improved dark-object substraction technique for atmospheric scattering correction of multispectral data. Remote Sensing of Environnement, 24, 459-479.

Doxani G, Papadopoulou M, Lafazani P 2012 Shallow water bathymetry over variable bottom types using multispectral worldview-2 image. The International Archives of the Photogrammetry, Remote Sensing and Spatial Information Sciences 391: 159–164.

Evagorou E, Mettas C, Agapiou A, Themistocleous K, Hadjimitsis D 2019. Bathymetric maps from multi-temporal analysis of Sentinel-2 data: the case study of Limassol, Cyprus. Adv. Geosci., 45, 397–407.

Hala ME, Dina SA, Mohammed AS2018. Derivation of Bathymetry Models for Shallow Water Using Multispectral Sentinel-2A Images for Delta Coast of Egypt. Res. J. Appl. Sci. Eng. Technol., 152: 81-90.

Hamylton, S. M., Hedley, J. D. and Robin J. Beaman. 2015. Derivation of High-Resolution Bathymetry from Multispectral Satellite Imagery: A Comparison of Empirical and Optimisation Methods through Geographical Error Analysis. Remote Sens., 7, 16257–16273.

Hauhouot C, N'doufou C2009. Dynamique sédimentaire du littoral ivoirien entre Grand-Lahou et Abidjan. Revue de Géographie Tropicale et d'Environnement, EDUCI, n° 2.

Jagalingam P, Akshaya BJ, Hegde AV 2015. Bathymetry Mapping Using Landsat 8 Satellite Imagery. Procedia Engineering 116 2015 560-566.

Jawak SD, Vadlamani SS,Luis AJ 2015. A Synoptic Review on Deriving Bathymetry Information Using Remote Sensing Technologies: Models, Methods and Comparisons. Advances in Remote Sensing, 4, 147-162.

Komoé K, Da KP, Kouassi AM, Aka NM, Kamanzi AK, Ama AA, 2009. Seasonal Distribution of Phytoplankton in Grand-Lahou Lagoon. European Journal of scientific Research 21 3: 329-341.

Kyriakidis PC, Dungan JL 2001. A geostatistical approach for mapping thematic classification accuracy and evaluating the impact of inaccurate spatial data on ecological model predictions. Environ. Ecol. Stat. 8, 311–330.

Lyzenga DR1978. Passive Remote Sensing Techniques for Mapping Water Depth and Bottom Features. Applied Optics, 17:3, 379-383.

Minghelli-Roman A, Goreac A, Mathieu S, Spigai M, Gouton P 2009. Comparison of Bathymetric Estimation Using Different Satellite Images in Coastal Sea Waters. *International Journal of Remote Sensing*, 30, 5737–50.

Stumpf RP, Holderied K, Sinclair M2003. "Determination of water depth with high-resolution satellite imagery over variable bottom types," *Limnol. Oceanogr.*, vol. 48, no. 1, pp. 547–556, 2003.

Su H, Liu H, Heyman WD, Filippi MA, Wang L, Beck RA 2014. Geographically Adaptive Inversion Model for Improving Bathymetric Retrieval from Satellite Multispectral Imagery. IEEE Transactions on Geoscience and Remote Sensing 521: 465–476.

Wognin V, Mondé S, Coulibaly A, Kouassi KL, Adopo L, Affian K, Aka K2008. Waters Model Circulation in the Estuary of Bandama. Rivers Flows and Tide Condition's Incidence, European Journal of Scientific Research ISSN 1450-216X Vol.19 No.2, pp.304-314.

Zhang Z, Ji M, Deng Z 2008. Mapping Bathymetry from Multi-Source Remote Sensing Images: A Case Study in the Beilun Estuary, Guangxi, China. The International Archives of the Photogrammetry, Remote Sensing and Spatial Information Sciences. Vol. XXXVII. Part B8.


*******